Scientific Research Publishing

Advances in Chemical Engineering and Science, 2022, 12, 145-162
https://www.scirp.org/journal/aces
ISSN Online: 2160-0406
ISSN Print: 2160-0392

Performance Evaluation of Ionic Liquids Using Numerical Simulation

Mostafa Elaghoury, Ali Alarbah, Ezeddin Shirif*, Na Jia

Petroleum Systems Engineering, University of Regina, Regina, Canada
Email: *ezeddin.shirif@uregina.ca

How to cite this paper: Elaghoury, M., Alarbah, A., Shirif, E. and Jia, N. (2022) Performance Evaluation of Ionic Liquids Using Numerical Simulation. *Advances in Chemical Engineering and Science*, **12**, 145-162.
https://doi.org/10.4236/aces.2022.123011

Received: March 27, 2022
Accepted: June 26, 2022
Published: June 29, 2022

Abstract

Given the rise in oil productivity from conventional and unconventional resources in Canada using Enhanced Oil Recovery (EOR), the need to understand and characterize these techniques, for the purpose of recovery optimization, has taken a prominent role in resource management. Chemical flooding has proved to be one of the most efficient EOR techniques. This study investigated the potential of employing Ionic Liquids (ILs) as alternative chemical agents for improving oil recovery. There is very little attention paid to employing this technique as well as few experimental and simulation studies. Consequently, very limited data are available. Since pilot and field studies are relatively expensive and time consuming, a numerical simulation study using CMG-STARS simulator was utilized to explore the efficiency of employing 1-Ethyl-3-Methyl-Imidazolium Acetate ([EMIM][Ac]) and 1-Benzyl-3-methlimidazolium chloride ([BenzMIM][Cl]) with respect to improving medium oil recovery. Eight different lab-scale sandpack flooding experiments were selected to develop a numerical model to obtain the history matching of the experimental flooding results using CMG-CMOST. We observed that the main challenge was tuning the relative permeability curves to achieve a successful match for the oil recovery factor. Finally, a sensitivity study was performed to examine the effect of the chemical injection rate, the chemical concentration, the slug size, and the initiation time on oil recovery. The results showed a noticeable increase in the oil RF when injecting IL compared to conventional waterflooding.

Keywords

CMG-STARS, CMG-CMOST, Chemical Flooding, Ionic Liquid, Recovery Factor, History Matching

1. Introduction

Considering the large quantities of oil remaining entrapped in the reservoir, re-

searchers are dedicated to developing new methods to increase oil production. When the primary recovery fails and a reservoir loses its natural energy to push the oil to the surface, other techniques known as such as a secondary oil recovery or improved oil recovery (IOR) come into play. Generally, the secondary recovery techniques are used to maintain reservoir pressure by fluid injection. There are different types of fluids that can be injected into the reservoir such as water and gases. In many cases, using the secondary recovery method is insufficient to recover the oil from the reservoirs. In order to increase oil recovery, other techniques known as tertiary or enhanced oil recovery (EOR) are utilized.

For many decades, EOR techniques have proven to be very efficient in increasing oil recovery. Generally, EOR can be divided into three categories: miscible flooding, thermal recovery, and chemical flooding which is the main focus of this research work. Chemical flooding includes injecting chemicals into the porous media to alter the reservoir characteristics such as reducing the interfacial tension of the system, altering the reservoir wettability and increasing the capillary number, decreasing the oil viscosity, or maintaining the mobility control. Three main chemical enhanced oil recovery methods have been reported in the literature: a polymer augmented waterflooding, an alkaline-polymer waterflooding (AP) and an alkaline-surfactant-polymer flooding (ASP).

Relatively new chemicals called Ionic Liquids (ILs) have been recently applied as chemical flooding agents in a lab-scale. ILs are composed of an organic cation and organic or inorganic anion, thermally stable with high conductivity. They have many advantages over other chemicals such as non-corrosiveness, low toxicity, and commercial availability [1]. Many laboratory studies have been conducted leading to a substantial increase in the number of synthesized ILs. Changing the size, shape, organization, and nature of anions and cations forming the ILs results in changing the chemical-physical properties such as miscibility [2]. Due to the high cost of ILs, they are mixed with water before being injected into the porous medium. The solubility of ILs in water depends on the hydrophilicity which can be manipulated by changing the anions and cations.

In recent years, many researchers became focused on investigating the potential of using ILs in the oil industry. Fathei *et al.* (2014) showed that injecting high concentration of ILs resulted in increasing the extracted oil from sandstone and carbonate reservoirs [3]. Lago *et al.* (2013) reported that Trihexyl (tetradecyl) phosphonium chloride IL increases the water viscosity and reduces the mobility ratio [4]. Hezave *et al.* (2013) measured the dynamic interfacial tension in medium oil/high salinity formation brine/[DMIM][Cl] systems. The authors reported a reduction in the IFT and an increase in the oil recovery by 13 [% OOIP] [5]. Also, Bin-Dahang *et al.* (2014) injected a mixture of Ammonium-based ILs with brine in a core sample; results showed an increase in oil recovery by 4.5 [% OOIP] due to change in the rock wettability towards water-wet [6]. In a similar study, the authors reported that ILs modified the wettability of the oil-wet limestone and sandstone more efficiently than injecting surfactants [7]. Pereira *et al.* (2014) conducted several core flooding experiments using ILs and found that

the highest recovery was achieved by injecting 1-ethyl-3-methylimi-dazolum tosylate ([C_2MIM][OTS]), which recovered 65.7% of trapped oil; approximately 30 [% OOIP] increase compared to applying conventional waterflooding process. The authors also investigated the ability of [EMIM][Ac] to improve the oil RF compared to other commercial surfactants. They injected nearly 4.02 PVs of the [SDS] + 1 wt% [NaCl] mixture and the [EMIM][Ac] + 1 wt% [NaCl] mixtures following conventional waterflooding. The additional oil recovery obtained were 8.54 and 10.55 [% OOIP] respectively. The results showed that [EMIM][Ac] was more efficient than sodium dodecyl sulfacte [SDS] and the efficiency of the displacing mixture was improved due to the increase in zeta potential value [8].

Tunnish *et al.* (2016) used a thermodynamic model COSMO-RS to conduct a screening study to examine different types of ILs with other phases. After conducting a selection study, the authors reported that injecting a low salinity aqueous solution of 1-Ethyl-3-methyl-Imidazolium Acetate [EMIM][Ac] increased heavy oil (14˚API) recovery compared to a polymer-augmented waterflooding [9]. Bin-dahbag *et al.* (2016) conducted three simulation runs to simulate lab scale core flooding experiments using IL and heavy oil by changing the injection scenarios. The authors found that tertiary flooding using IL solution yielded nearly additional 5 [% OOIP] compared to waterflooding. The authors also reported that IL was able to alter the rock wettability [10]. In another study, 2-acrylamido-2-methylpropoane sulfonic acid copolymer with methacrylic acid (AMPSA/MAA) in a low water salinity (3000 ppm) were screened among other polyionic liquids (PILs) at different concentrations and proved to be the most effective chemical recovery agent as it resulted in increasing oil recovery by nearly 10 [% OOIP] [11]. Alhussianan *et al.* (2018) extended the study of ILs to explore the effect of PIL AMPSA/MA on carbonates. A post secondary flooding with 3000 ppm of 0.4 PV slug of AMPSA/MAA PIL was injected into the core sample and flushed with seaweater. The PIL injection resulted in an increment of 6 [% OOIP] compared to 10% obtained from sandstone. The authors investigated the mechanism of oil recovery by measuring the IFT and concluded that the IFT drop was the main mechanism for oil recovery from carbonates [12]. Alarbah *et al.* (2019) investigated the efficiency of 1-Ethyl-3-methylimidazolium Chloride [EMIM][Cl] on oil recovery. The authors reported a noticeable increase in oil recovery due to reduction in mobility ratio and surface tension of displacing fluids and that IL used had the ability to improve the wettability of the rocks to become more water-wet [13].

To the best of the authors' knowledge, there has not been any study of ILs in a field scale. Therefore, a simulation model which as powerful tool to gain insight into reservoir performance was used to study the ILs flooding. The goal for using a simulator is to build a numerical model which matches the experimental results. Once a history matching is achieved, different conditions and scenarios can be investigated, and the information acquired can be used to forecast oil production.

2. Methodology

To develop an understanding of the chemical flooding using ILs, we built a simulation model using the results of eight lab-scale core flooding experiments. Computer Modelling Group LTD. (CMG) STARS was adopted as the simulator for this research. CMG was selected because the simulator has the capacity and functionality required to model chemical flooding and the simulator is commonly used in the industry. History matching was conducted by tuning the relative permeability using CMG-CMOST. Once history matching was achieved, a sensitivity analysis was conducted to study the effect of different parameters on the chemical flooding using ILs and the optimum case is presented. Also, the results showing increase of oil recovery using ILs were supported from the findings of the IFT measurements.

2.1. Description of the Numerical Model

The grid modeling was performed on the basis of the cartesian grid system to describe the sandpack. To simplify, the core sample was assumed to have a cuboidal shape instead of a cylindrical shape with the same volume and same cross-sectional area of the cylinder used in the laboratory. The cuboidal was divided into 80 blocks in the X-axis in the flow direction to increase the model precision, 1 block (3.54 cm in width) in the Y-axis and 1 block (3.54 cm in height) in the Z-axis to simulate 1-D flow. The optimum number of grid blocks was determined based on the truncation error. The null properties were given to grid blocks outside the model boundaries. The total number of grid blocks in effect was 80 with the model pressure. One injector well was placed in block 1, 1, 1 while the producer well was placed in block 80, 1, 1. The diameter of the well was 0.4 cm. Figure 1 displays the grid system used in this model.

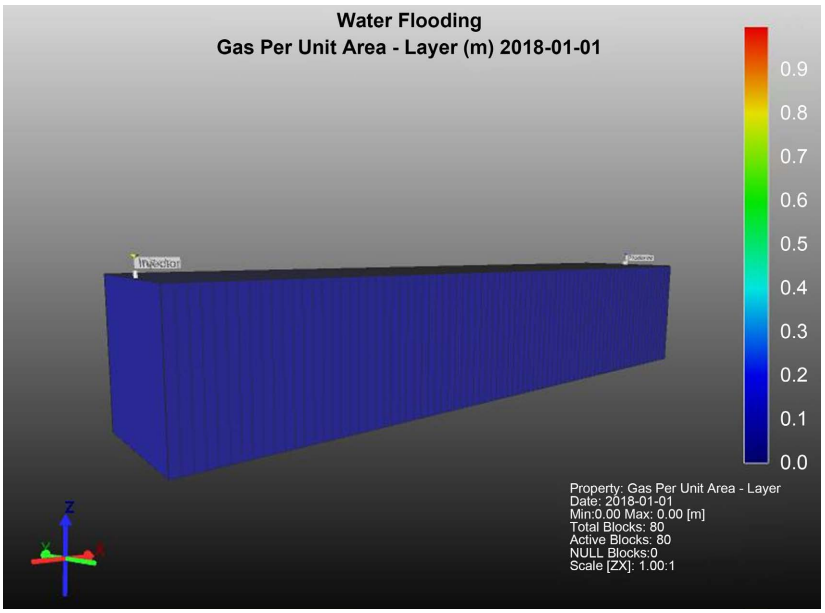

Figure 1. Cartesian grid design for numerical model.

2.2. Reservoir Properties

The relevant core sample physical property data were obtained from the laboratory experiments [14] and supplemented with CMG templates if needed. A summary of the rock and fluid properties is shown in Table 1.

2.3. Relative Permeability

The reservoir model used is a water-wet sandstone medium. The two-phase relative permeability for the base case utilized in this study is based on the laboratory flooding experiments [14]. The two-phase water oil relative permeability as a function of water saturation is shown in Table 2. It should be stated that the formation compressibility utilized in the model was 4×10^{-5} [1/kPa] with the porosity reference pressure at 101.3 kPa.

2.4. Tuning of Water-Oil Relative Permeability Curves

In this study, Cory's correlations (Equation (1) and (2)) were utilized to obtain

Table 1. Rock and fluid properties.

Rock Properties		Fluid Properties	
Grid Size (x), cm	0.234	Water Density, g/cm^3	1.066
Grid Thickness, cm	3.54	Water Viscosity, cP	1.017
Grid	80	Oil Density, g/cm^3	0.874
K_x, K_y, K_z, mD	5100	Oil API°	30.25
Φ, %	40	Oil Viscosity, cP	15.35
Reservoir Pressure, kPa	101.3	Initial Oil Saturation, %	83
Rock Type	Sandstone	Initial Water Saturation, %	17

Table 2. Water oil relative permeability.

S_w	k_{rw}	K_{ro}
0.17	0.0000	0.6959
0.23	0.0202	0.5913
0.27	0.0330	0.5201
0.32	0.0465	0.4379
0.37	0.0596	0.3709
0.47	0.0865	0.2345
0.57	0.1118	0.1255
0.67	0.1462	0.0569
0.71	0.1674	0.0343
0.75	0.1861	0.0156
0.79	0.2100	0.0000

history matching for the experimental results. In some cases, the relative permeability curves had to be adjusted in part manually, alongside Corey's correlations to achieve successful history matching results.

$$K_{rw} = K_{rwiro}\left(\frac{S_w - S_{wcrit}}{1 - S_{wcrit} - S_{oirw}}\right)^{N_w} \quad (1)$$

$$K_{row} = K_{rocw}\left(\frac{S_o - S_{orw}}{1 - S_{wcon} - S_{orw}}\right)^{N_{ow}} \quad (2)$$

where K_{rw}: water relative permeability; K_{rwiro}: water relative permeability at irreducible oil; S_w: water saturation; S_{wcrit}: critical water saturation; K_{row}: oil relative permeability; K_{rocw}: oil relative permeability at connate water saturation; S_o: oil saturation; S_{orw}: residual oil saturation; S_{wcon}: connate water saturation; N_w: water relative permeability curve exponent and N_{ow} oil relative permeability curve exponent.

In the application of Corey's equation, the exponents, N_w and N_{ow} were adjusted first. Then endpoints, critical water saturation and residual oil saturation, were adjusted if necessary.

2.5. Interfacial Tension Measurements

Pendant drop tensiometer with advanced image software was used to measure the interfacial tension (IFT) between the displacing and displaced phases. The experimental setup shown in Figure 2, consists of three parts: 1) an experimental cell (IFT-10, Temco), 2) illuminating and viewing system to visualize the drop and 3) a data acquisition system to calculate the interfacial tension from a pendant drop profile. The pendant drop was measured by filling the cell with the aqueous solution/mixture. Then the oil droplet at the tip of the needle was injected into the solution and after allowing enough time to reach stability, the IFT measurement was taken. Although the pendant drop apparatus is relatively simple, a number of factors must be considered to ensure the quality of the drop and to achieve a precise determination of the interfacial tension. For instance, the equilibrium time is crucial for measurement accuracy which depends on the oil grade [15]. Furthermore, the volume of the injected drop plays a significant role

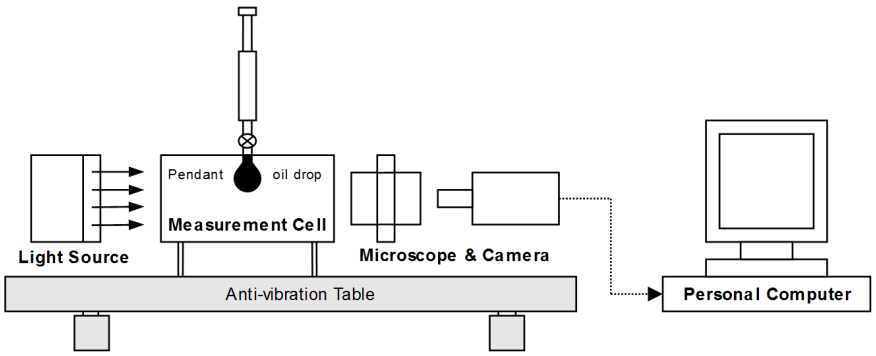

Figure 2. Schematic of the experimental setup used to measure IFT.

in measurement precision and should be kept within the range of 7 to 30 µl [16].

The rationale for using the pendant drop is that it is considered to be the most convenient, versatile and popular method to measure the IFT. It involves the determination of the profile of a drop of one liquid suspended in another liquid at mechanical equilibrium resulting from the balance between gravity and surface forces. The pendant drop at equilibrium confirms to the Young-Laplace equation, which related the Laplace pressure across an interface with the curvatures of the interface and the interfacial tension [17]:

$$\gamma\left(\frac{1}{R_1}+\frac{1}{R_2}\right)=\Delta P\equiv\Delta P_0-r\varphi\Delta\rho gz \tag{3}$$

where R_1 and R_2 are the principal radii of curvature; $\Delta P=P_{in}-P_{out}$: is the Laplace pressure across the interface; $\Delta\rho=\rho_d-\rho$: is the density difference; and ρ_d and ρ are the drop phase density and the continuous phase density respectively.

Figure 3 displays the variations of the IFT with [EMIM][AC] concentration in brine. This figure shows a sharp decline in IFT after adding the [EMIM][AC] up to 1000 ppm which indicates that the critical micelle concentration (CMC) of [EMIM][AC] is 1000 ppm. The CMC is the concentration at which the IL starts to self aggregate and form micelles; resulting in no further reduction in the IFT. When the IL concentration is lower than CMC, the IL molecules lay on the surface. Then by increasing the IL concentration toward CMC, the IL molecules start to form a monolayer which leads to a reduction in both the interfacial energy and interfacial tension. In a similar study Pereira *et al.* (2014) showed that

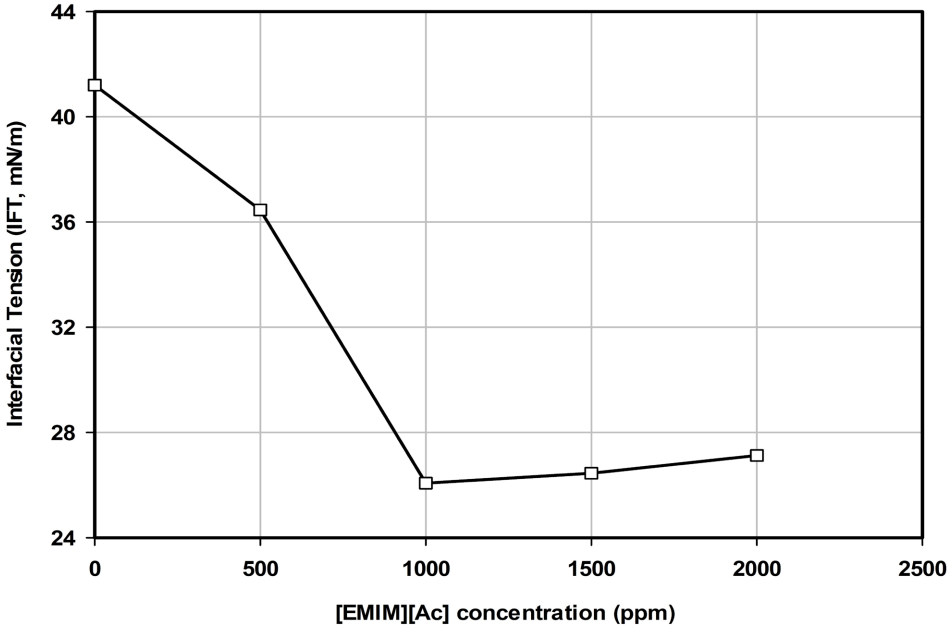

Figure 3. Effect of [EMIM][Ac] concentration on IFT of crude oil/[EMIM][Ac] solution at ambient conditions.

IL (1-ethyl-3-methylimidazolium tosylate [C_2mim][OTs]) decreased the IFT between medium oil and brine from 19.2 to 17.0 mN/m [8].

A different type of IL known as [BenzMIM][Cl] was also tested and results show that the IFT for the system was reduced from 41.21 to 32.03 [mN/m] at the CMC concentration as shown in Figure 4. This proves that regardless of the IL type, they behave the same as surfactants and are able to reduce the energy level of the interface between the oil phase and aqueous phase and hence decrease the IFT [18]. Based on the results of the IFT measurements, [EMIM][Ac] at CMC concentration proved to be more efficient in reducing the IFT and consequently has a higher potential in improving oil recovery.

3. Results and Discussion

3.1. History Matching of Waterflooding Experimental Results (Base Case)

The saturated core sample was continuously flooded with 3 PVs of formation brine to form the base case. The history matching was conducted using CMOST. Relative permeability was the parameter utilized to obtain history matching. Corey's correlation for relative permeability was used by CMOST in which only water and oil exponents were varied. The cumulative oil production profile obtained from CMOST is shown in Figure 5. The relative permeability end point is 0.21, which is relatively low, and the formation rock is strong water wet as shown in Figure 6. However, it is expected that the rock be less water wet as it was observed during the experiment. This could potentially be due to the difference in the area utilized for fluid flow in simulation and experiment.

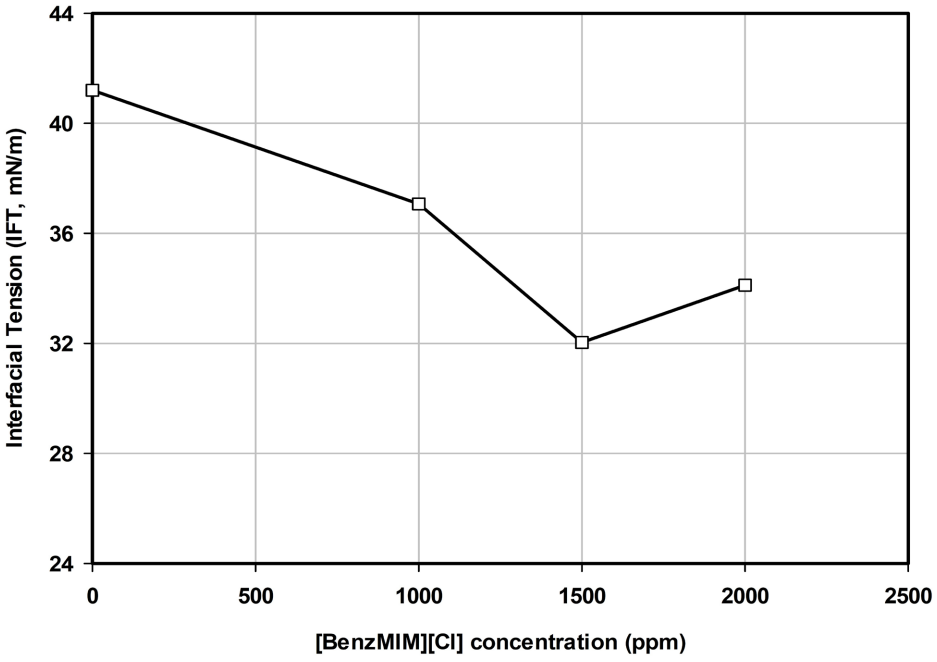

Figure 4. Effect of [BenzMIM][Cl] concentration on IFT of crude oil/[BenzMIM][Cl] solution at ambient conditions.

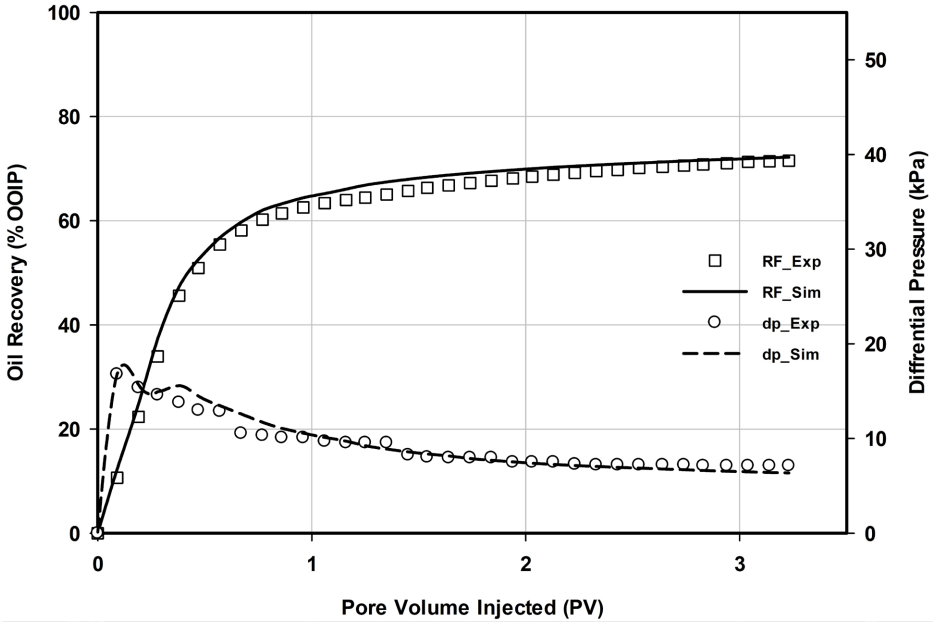

Figure 5. History matching results of oil recovery and differential pressure (Base Case).

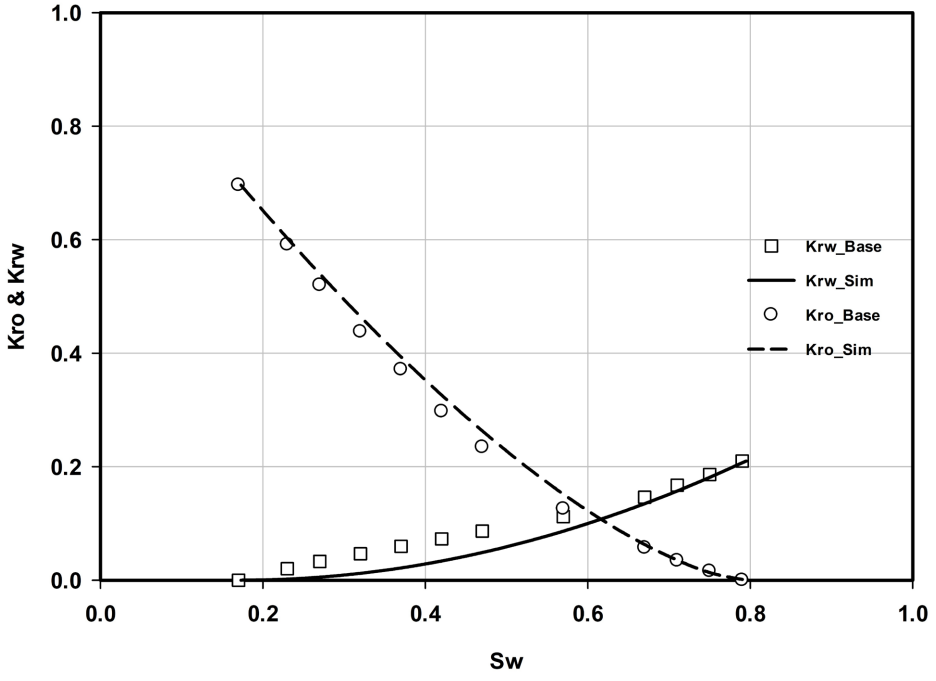

Figure 6. Tuned water-oil relative permeability curve (Base Case).

3.2. History Matching of Ionic Liquids Flooding Experimental Results

Two experiments were selected for this analysis. First, the saturated core sample was injected by 1 PV of formation water followed by 1 PV of [EMIM][Ac] with a concentration 1000 ppm then flushed with 1 PV of brine. Second, the saturated core sample was initially flooded with 1 PV of brine then flooded with 1 PV of [BenzMIM][Cl] with a concentration of 1500 ppm then flushed with 1 PV of brine.

For the first run, the values for simulated and experimental oil recovery for the IL flooding are 78.28 and 77.21 [% OOIP], respectively as shown in Figure 7. The simulation results showed that the IL was able to recover additional 6.49 [% OOIP] compared to the base case. The oil saturation substantially decreased from 0.83 at the beginning of the water flooding to 0.16 at the end of the IL solution flooding. This increase in oil recovery can be explained by the change in rock wettability as illustrated by the imbibition relative permeability curve in Figure 8. The intersection points of the water and oil relative permeability curves for IL

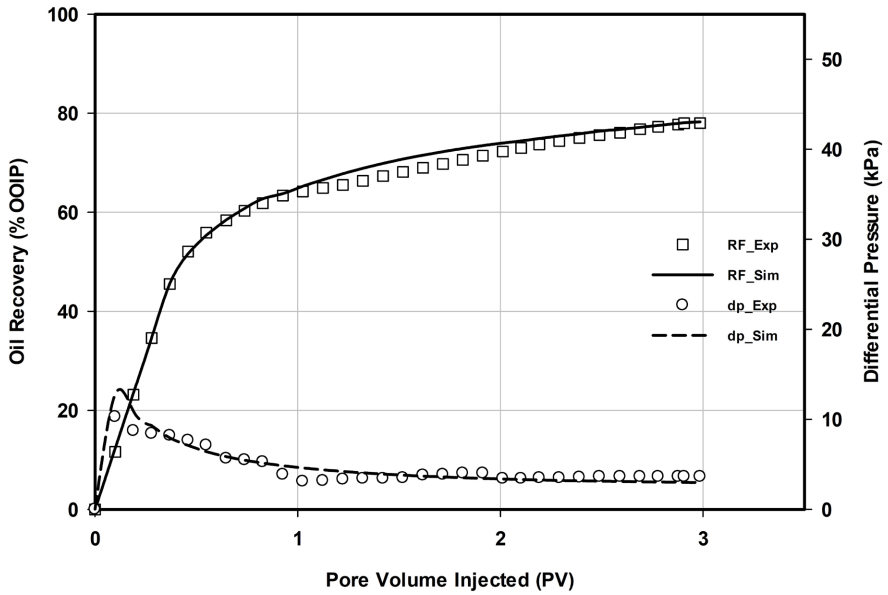

Figure 7. History matching results oil recovery and differential pressure (Brine + 1000 ppm [EMIM][Ac]).

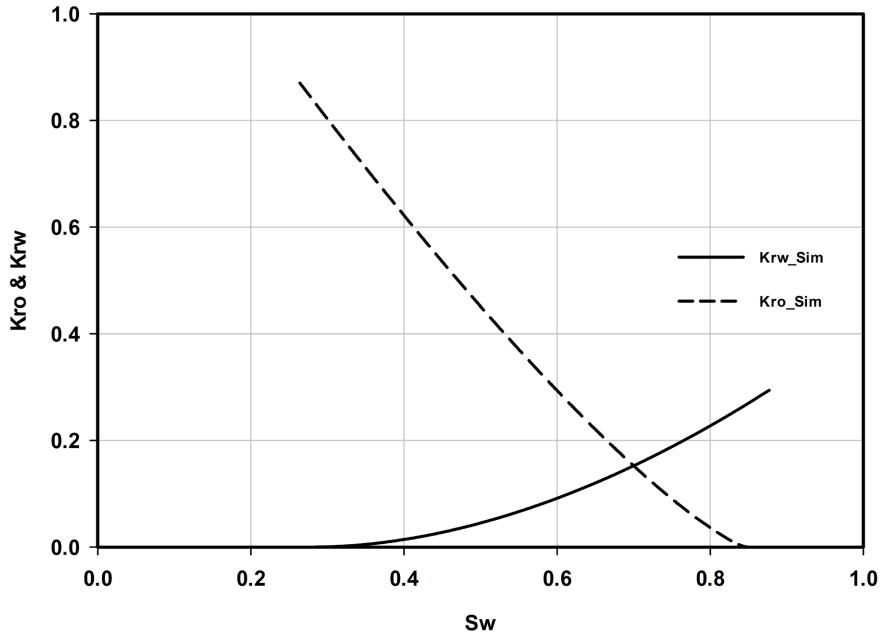

Figure 8. Water-oil relative permeability curve (Brine + 1000 ppm [EMIM][Ac]).

flooding and base case are 0.69 and 0.62, respectively. These results are supported by the reduction in the IFT as illustrated in the experimental measurements. Generally, the IFT reduction and the wettability alteration are thought to be the most probable mechanisms leading to improvement in oil recovery by IL flooding. This is also in agreement with another study where increasing the concentration of the IL (Ammoeng 102) resulted in decreasing the contact angle of the oil droplet and changed the rock wettability from oil-wet to medium water-wet [8]. Finally, the viscosity of [EMIM][Ac] slightly increased the viscosity of the displacing phase and can be considered as one of the reasons for improving oil RF.

The main objective of the second run was to investigate the efficiency of different types of ionic liquids on oil recovery. After a conventional water flooding, 1 PV of 1500 ppm of [BenzMIM][Cl] was injected into the core sample followed by 1 PV of chase water to flush the core sample. Results show an increment of oil RF by nearly 4.33 [% OOIP] compared to the base case as shown in Figure 9. On the other hand, in comparison with the [EMIM][Ac], the incremental RF of the same chemical slug decreased by 2.16 [% OOIP]. This reduction in the oil RF is also in agreement with the results from the IFT measurements in which the [EMIM][Ac] was more efficient in reducing the system IFT than [BenzMIM][Cl]. Therefore, [EMIM][Ac] is considered the optimum IL type and was utilized for the rest of the simulation runs in this study.

3.3. Sensitivity Studies

The sensitivity analysis is a critical part of any simulation study because it allows the engineer to conduct different scenarios that could be cost prohibitive in the

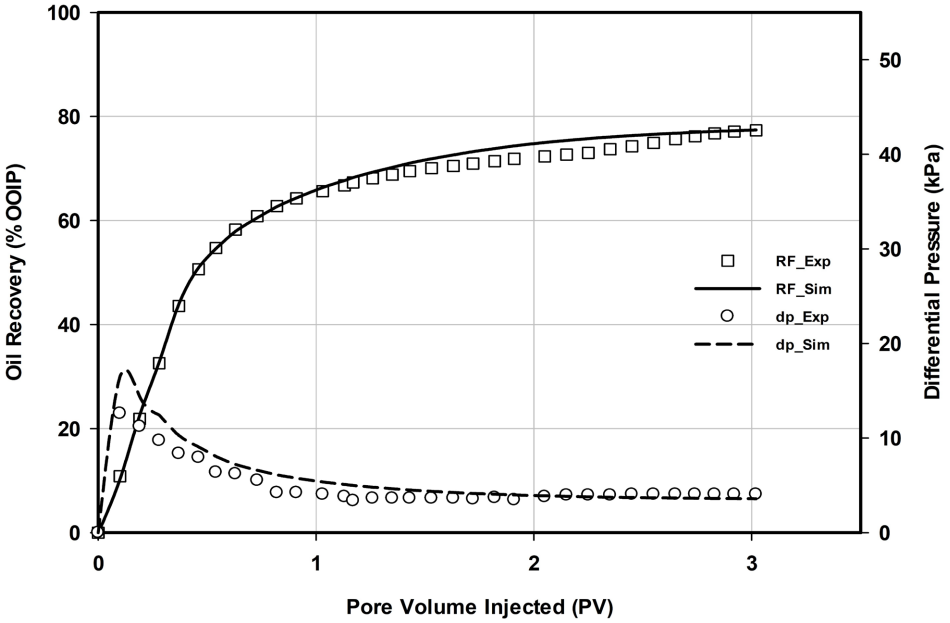

Figure 9. History matching results oil recovery and differential pressure (Brine + 1500 ppm [BenzMIM][Cl]).

laboratory. In this study, the effect of changing the fluid injection rate, concentration of chemicals, chemical slug size, and chemical initiation time on oil RF is tested.

Effect of Injection Rate

In any flooding process, the displacing fluid injection rate has a direct effect on the production efficiency. Therefore, determining the optimum injection rate is necessary to achieve a successful and cost-effective flooding job. The displacing fluid injection rate was planned in the range of 0.1 cm^3/min to 4 cm^3/min for the [EMIM][AC] slug. As shown in Figure 10, changing the injection rate of the

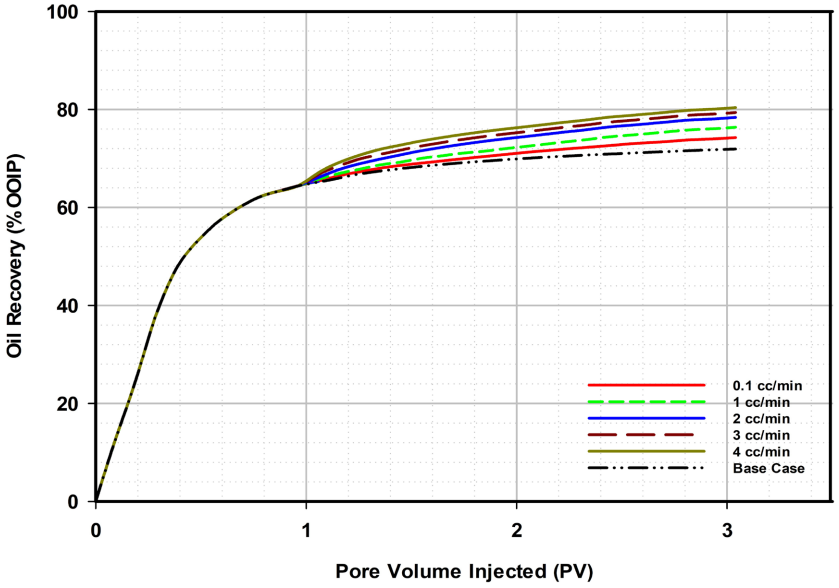

(a)

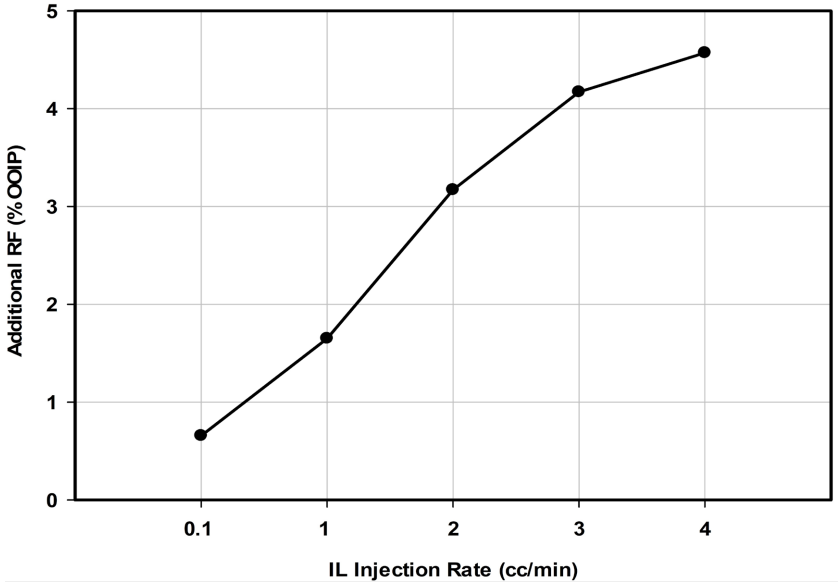

(b)

Figure 10. Effect of changing [EMIM][AC] injection rate on oil RF (a) simulation results (b) cross plot of additional RF after 1.5 PV.

displacing fluid resulted in a significant change in the cumulative oil recovery. Compared to the base case, the additional oil RF resulted from injection rates of 0.1 cm^3/min and 4 cm^3/min are 0.66 and 4.57 [% OOIP], respectively. However, the difference in additional oil RF between 2 cm^3/min and 4 cm^3/min was nearly 1.43 [% OOIP] which does not justify the high consumption of chemical needed as a result of increasing the injection rate. Therefore, 2 cm^3/min is considered the optimum [EMIM][AC] injection rate in this study.

Effect of Chemical Concentration

The effect of [EMIM][AC] concentration on oil RF was investigated by employing a concentration range of 100 to 10,000 ppm. As shown in **Figure 11**, increasing the [EMIM][AC] concentration from 100 to 1000 ppm resulted in a noticeable increase in additional oil RF compared to the base case which is in agreement with the IFT measurements where the value of the system IFT drastically decreased as the concentration increased to 1000 ppm. However, increasing the [EMIM][AC] concentration from 1000 to 3000 ppm resulted in nearly the same additional oil RF because 1000 ppm is considered the CMC for [EMIM][Ac] and increasing the concentration beyond this point, resulted in slight decrease in the system IFT. On the other hand, increasing the concentration to 10,000 ppm resulted in a substantial increase in the oil RF. This could be explained by the increase in the viscous force and a reduction in the mobility ratio when the concentration is very high. Although applying a concentration of 10,000 ppm resulted in a noticeable increase in additional oil recovery by nearly 2.19 [% OOIP] compared to 1000 ppm, economically speaking, using very high concentration is not practical due to the high cost of IL. Therefore, 1000 ppm concentration of [EMIM][AC] is considered the optimum case.

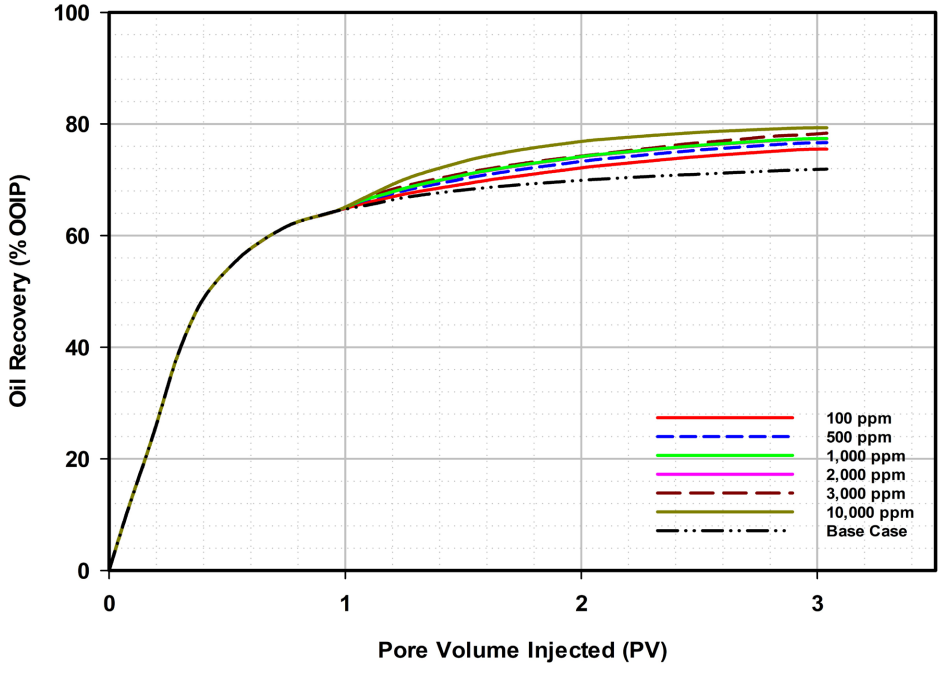

(a)

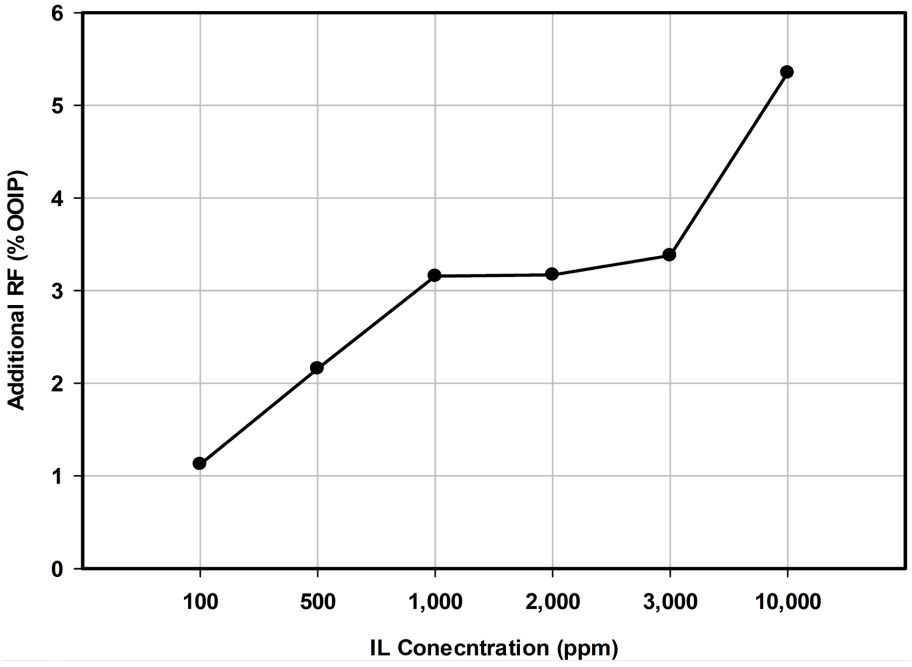

(b)

Figure 11. Effect of changing [EMIM][AC] concentration on oil RF (a) simulation results (b) cross plot additional RF after 1.5 PV.

Effect of Chemical Slug Size

Similar to displacing fluid injection rate, the chemical slug size has a significant impact on the economics of the chemical flooding process. Five different slug sizes of 1000 ppm of [EMIM][AC] were investigated as illustrated in **Figure 12**. Initially, conventional waterflooding (1 PV) was utilized followed by the different sizes of IL, then flushed with chase water until the end of the simulation run. The results show that the additional oil RF increased from 0.59 to 3.12 [% OOIP] as the IL slug size increased from 0.2 to 1 PV while it increased by nearly 1.21 as the slug size was raised from 1 to 2 PV. It is clear that increasing the [EMIM][AC] slug size beyond 1 PV does not increase the oil RF economically and hence 1PV is selected as the optimum slug size in this study.

Effect of Chemical Initiation Time

In order to determine the optimum [EMIM][AC] initiation time, 4 different scenarios were investigated to determine the effect of initiation time on oil RF. 1 PV of [EMIM][AC] was initially introduced to the core sample followed by brine and then planned to begin after 0.5 PV, 1 PV and 1.5 PV of waterflooding then flushed by brine until the end of the simulation run. **Figure 13** reveals that the cumulative oil RF is sensitive to the [EMIM][AC] initiation time. Results show that oil RF when [EMIM][AC] was introduced after 0 and 1.5 PV of brine flooding, are 81.70 and 75.54 [% OOIP], respectively. It is obvious that introducing the [EMIM][AC] at an early stage helped to improve the oil RF. However, from the economic perspective, this should be carefully designed based on the IL slug size utilized in order to achieve a cost-effective flooding job.

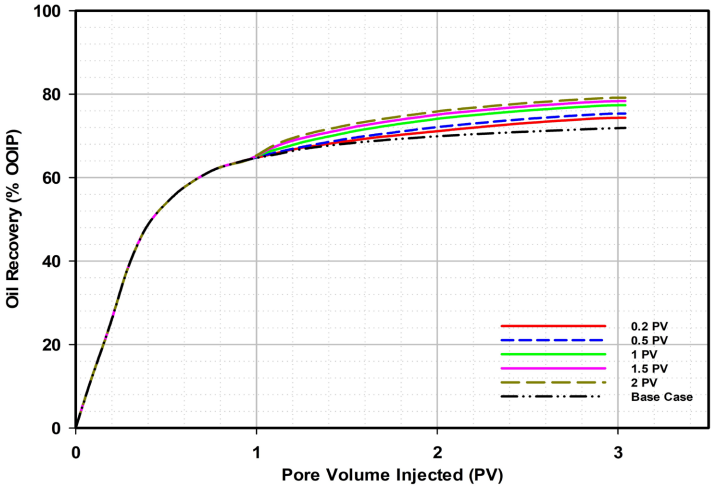

(a)

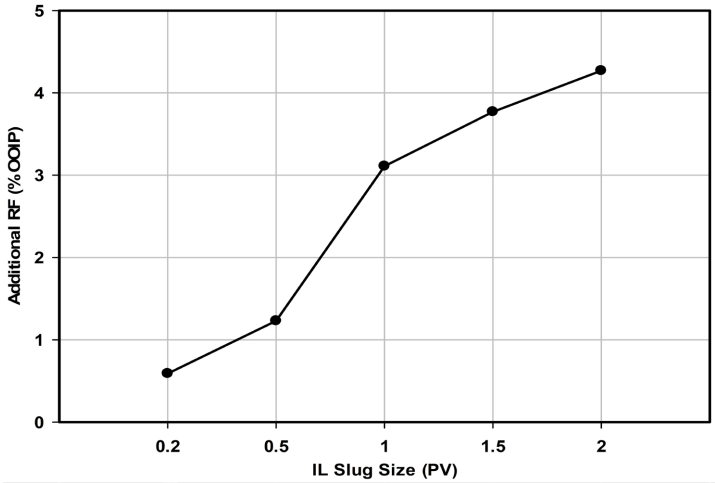

(b)

Figure 12. Effect of changing [EMIM][AC] slug size on oil RF (a) simulation results (b) cross plot of additional RF after 1.5 PV.

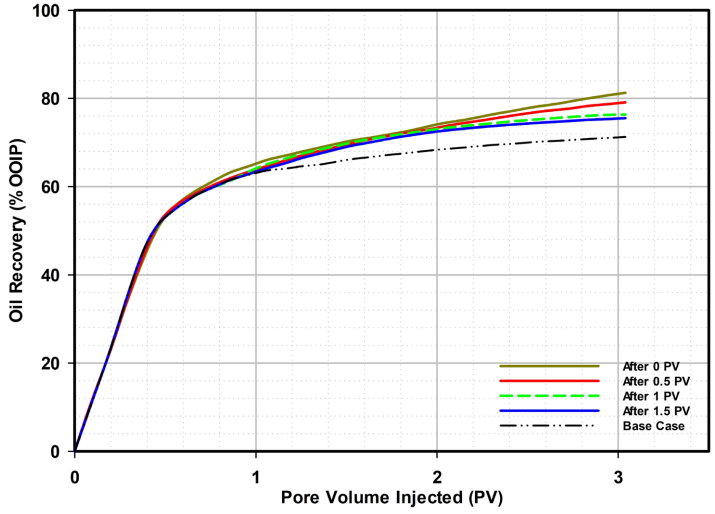

(a)

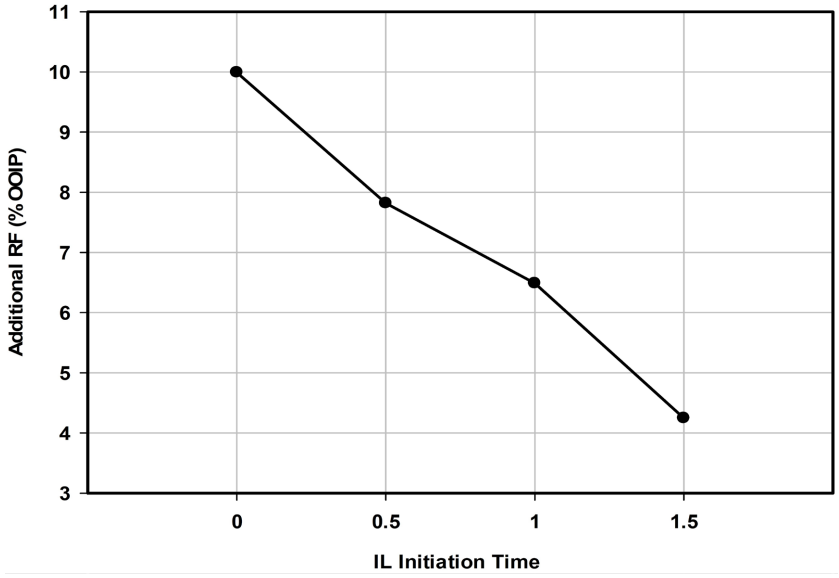

(b)

Figure 13. Effect of changing [EMIM][AC] initiation time on oil RF (a) simulation results (b) cross plot of additional RF after 3 PV.

4. Conclusion

Numerical simulation technique was employed to history match lab scale core flooding using ILs by utilizing CMG CMOST. The matched results of oil recovery and pressure drop curves proved the ability of CMG CMOST to successfully history match cumulative oil production profile by tuning the relative permeability curves using Corey's correlations, but less accurate in matching the differential pressure profile. Results from CMG STARS simulator showed the ability of both [EMIM][AC] and [BenzMIM][Cl] in reducing the IFT and altering the rock wettability towards water-wet. However, injecting [EMIM][AC] resulted in an additional oil RF of 6.49 [% OOIP] compared to 4.33 [% OOIP] when [BenzMIM][Cl] was injected using the same slug size. Sensitivity analysis showed that 1 PV is considered the optimum [EMIM][AC] slug size and increasing the [EMIM][AC] concentration beyond 1000 ppm resulted in a marginal increase in oil RF. Results also showed that changing the [EMIM][Ac] injection rate resulted in a significant change in the cumulative oil recovery. Furthermore, results showed that increasing the [EMIM][Ac] slug size from 0.2 to 1 PV led to additional oil recovery from 0.59 to 3.12 [% OOIP] and a 1 PV is considered the optimum slug size. Finally, this study pointed out that the IFT reduction and the wettability alteration besides increasing the viscosity of the displacing phase are thought to be the most probable mechanisms leading to improvement in oil recovery by IL flooding.

Conflicts of Interest

The authors declare no conflicts of interest regarding the publication of this paper.

References

[1] Quintriqueo, A., Romero, J., Quijada-Maldonado, E., Bringas, E., Olea, F. and Hernandez, J. (2020) Extraction and Separation Factor for Lanthanum (III) and Cerium (III) Complexes from Aqueous Medium Using Ionic Liquid and Kerosene. *Advances in Chemical Engineering and Science*, **10**, 343-357. https://doi.org/10.4236/aces.2020.104022

[2] Freire, M.G., Carvalho, P.J., Gardas, R.L., Marrucho, I.M., Santos, L.M.N.B.F. and Coutinho, J.A.P. (2008) Mutual Solubilities of Water and the [Cnmim][Tf2N] Hydrophobic Ionic Liquids. *The Journal of Physical Chemistry B*, **112**, 1604-1610. https://doi.org/10.1021/jp7097203

[3] Fathi, S.J., Austad, T. and Strand, S. (2011) Water-Based Enhanced Oil Recovery (EOR) by Smart Water Optimal Ionic Composition for EOR in Carbonates. *Energy & Fuels*, **25**, 5173-5179. https://doi.org/10.1021/ef201019k

[4] Lago, S., Francisco, M., Arce, A. and Soto, A. (2013) Enhanced Oil Recovery with the Ionic Liquid Trihexyl (Tetradecyl) Phosphonium Chloride: A Phase Equilibria Study at 75 ˚C. *Energy Fuels*, **27**, 5806-5810. https://doi.org/10.1021/ef401144z

[5] Hezave, A.Z., Dorostkar, S., Ayatollahi, S., Nabipour, M. and Hemmateenejad, B. (2013) Investigating the Effect of Ionic Liquid (1-Dodecyl-3-Methylimidazolium Chloride ([C 12 mim][cl])) on the Water/Oil Interfacial Tension as a Novel Surfactant. *Colloids and Surfaces A*: *Physicochemical and Engineering Aspects*, **421**, 63-71. https://doi.org/10.1016/j.colsurfa.2012.12.008

[6] Bin-Dahbag, M.S., Al Quraishi, A.A., Benzagouta, M.S., Kinawy, M.M., Al Nashef, I.M. and Al, E. (2014) Experimental Study of Use of Ionic Liquids in Enhanced Oil Recovery. *Journal of Petroleum & Environmental Biotechnology*, **4**, 1-7.

[7] Mohammed, M.A. and Babadagli, T. (2016) Experimental Investigation of Wettability Alteration in Oil-Wet Reservoirs Containing Heavy Oil. *SPE Reservoir Evaluation & Engineering*, **19**, 633-644. https://doi.org/10.2118/170034-PA

[8] Pereira, J.F., Costa, R., Foios, N. and Coutinho, J.A. (2014) Ionic Liquid Enhanced Oil Recovery in Sand-Pack Columns. *Fuel*, **134**, 196-200. https://doi.org/10.1016/j.fuel.2014.05.055

[9] Tunnish, A., Shirif, E. and Henni, A. (2016) Enhanced Heavy Oil Recovery Using 1-Ethyl-3-Methyl-Imidazolium Acetate. *The Canadian Journal of Chemical Engineering*, **95**, 871-879. https://doi.org/10.1002/cjce.22733

[10] Bin-Dahbag, M.S. and Hossain, E.M. (2016) Simulation of Ionic Liquid Flooding for Chemical Enhance Oil Recovery Using CMG STARS Software. SPE Kingdom of Saudi Arabia Annual Technical Symposium and Exhibition, Dammam, April 2016, 182836-MS.

[11] Abdullah, M.M., AlQuarishi, A.A., Allohedan, H.A., AlMansour, A.O. and Atta, A.M. (2017) Synthesis of Novel Water Soluble Poly (Ionic Liquids) Based on Quaternary Ammonium Acrylamidomethyl Propane Sulfonate for Enhanced Oil Recovery. *Journal of Molecular Liquids*, **233**, 508-516. https://doi.org/10.1016/j.molliq.2017.02.113

[12] Alhussinan, S.N., Alyami, H.Q., Alqahtani, N.B., AlQuarishi, A.A. (2018) Chemical Enhanced Oil Recovery with Water Soluble Poly Ionic Liquids in Carbonate Reservoirs. *SPE Kingdom of Saudi Arabia Annual Technical Symposium and Exhibition*, Dammam, April 2018. https://doi.org/10.2118/192373-MS

[13] Alarbah, A., Shirif, M. and Shirif, E. (2019) Investigation of Different Ionic Liquids in Improving Oil Recovery Factor. *Advances in Chemical Engineering and Science*,

9, 87-98. https://doi.org/10.4236/aces.2019.91007

[14] Alarbah, A., Shirif, M. and Shirif, E. (2017) Efficiency of Ionic Liquid 1-Ethyl-3-Methyl-Imidazolium Acetate [EMIM][AC] in Enhanced Medium Oil Recovery. *Advances in Chemical Engineering and Science*, **7**, 291-303. https://doi.org/10.4236/aces.2017.73022

[15] Kumar, B. (2012) Effect of Salinity on the Interfacial Tension of Model and Crude Oil Systems. MSc, University of Calgary, Calgary. https://doi.org/10.3997/2214-4609.20143757

[16] Buckley, J.S. and Fan, T.S. (2007) Crude Oil/Brine Interfacial Tensions 1. *Petrophysics*, **48**, 178-185.

[17] Berry, J.D., Neeson, M.J., Dagastine, R.R., Chan, D.Y.C. and Tabor, R.F. (2015) Measurement of Surface and Interfacial Tension Using Pendant Drop Tensiometry. *Journal of Colloid and Interface Science*, **454**, 226-237. https://doi.org/10.1016/j.jcis.2015.05.012

[18] Kelkar, M.S. and Maginn, E.J. (2007) Effect of Temperature and Water Content on the Shear Viscosity of the Ionic Liquid 1-Ethyl-3-Methylimidazolium Bis (Trifluoromethanesulfonyl) Imide as Studied by Atomistic Simulations. *The Journal of Physical Chemistry B*, **111**, 4867-4876. https://doi.org/10.1021/jp0686893